Supplement of Atmos. Chem. Phys., 22, 597–624, 2022
https://doi.org/10.5194/acp-22-597-2022-supplement

Atmospheric Chemistry and Physics
Open Access
EGU

Supplement of

Duff burning from wildfires in a moist region: different impacts on $PM_{2.5}$ and ozone

Aoxing Zhang et al.

Correspondence to: Yongqiang Liu (yongqiang.liu@usda.gov)

Supplementary Materials of "Duff burning from wildfires in a moist region: different impacts on $PM_{2.5}$ and Ozone"

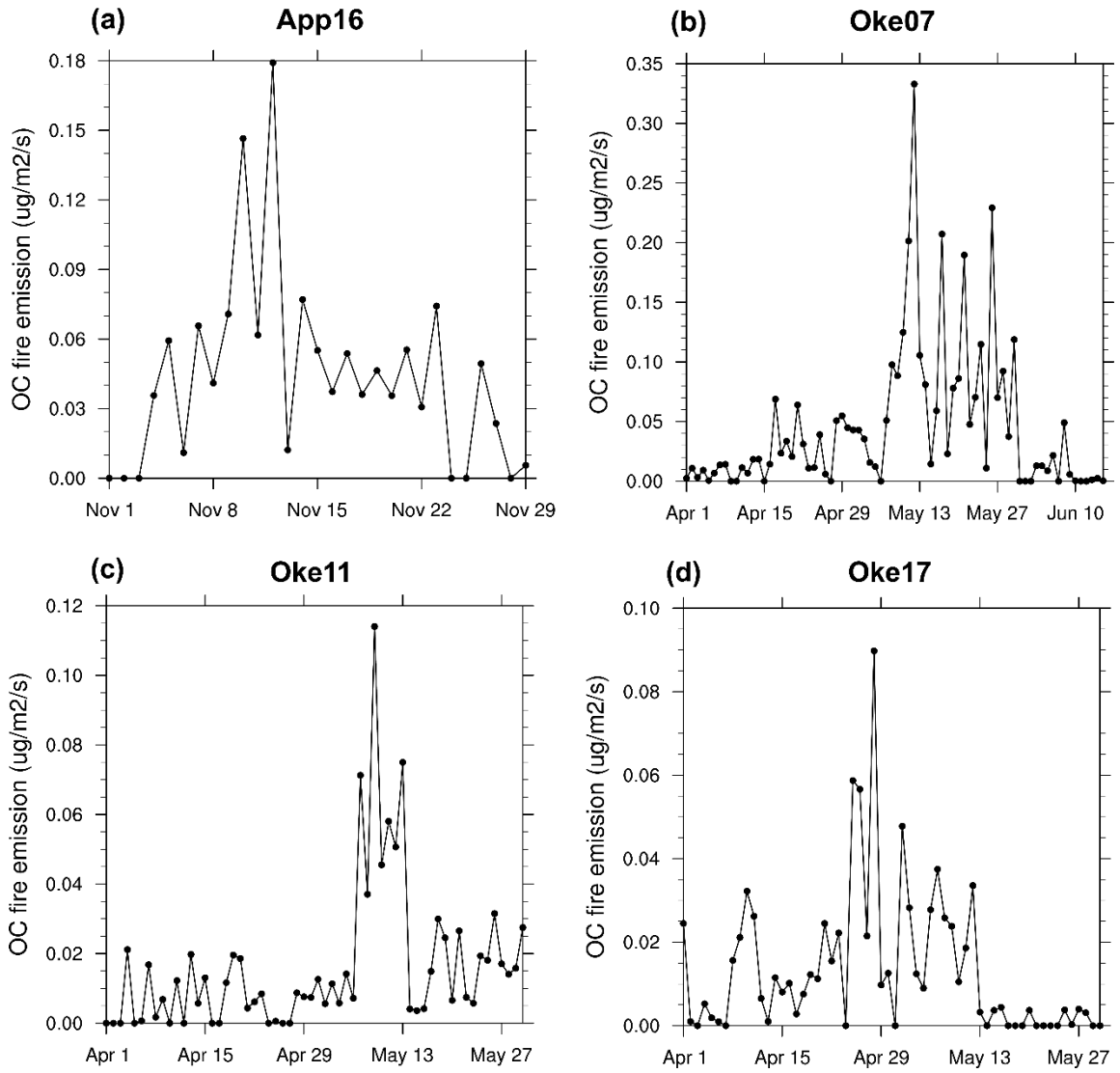

Figure S1. The daily trend of FINN fire emissions of organic carbon (OC) during the fire events. (a) the Southern Appalachian region (34.5° N to 36° N, 82° W to 84° W). (b) - (d) the Okefenokee region (30° N to 32° N, 81° W to 83° W).

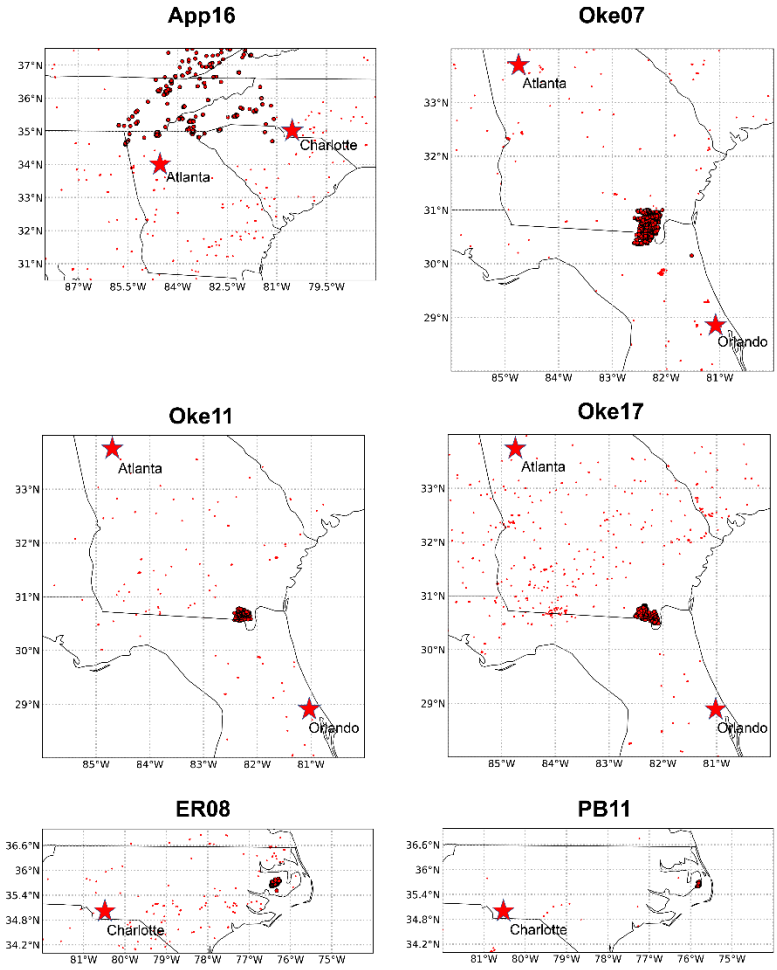

Figure S2. The burning hotspots from FINN emission inventory during the studied time periods for each case. The larger scatters represent the studied fire events with duff burning, and the smaller scatters represent the FINN hotspots with no duff burning. The nearby cities potentially affected by the studied fire cases are marked.

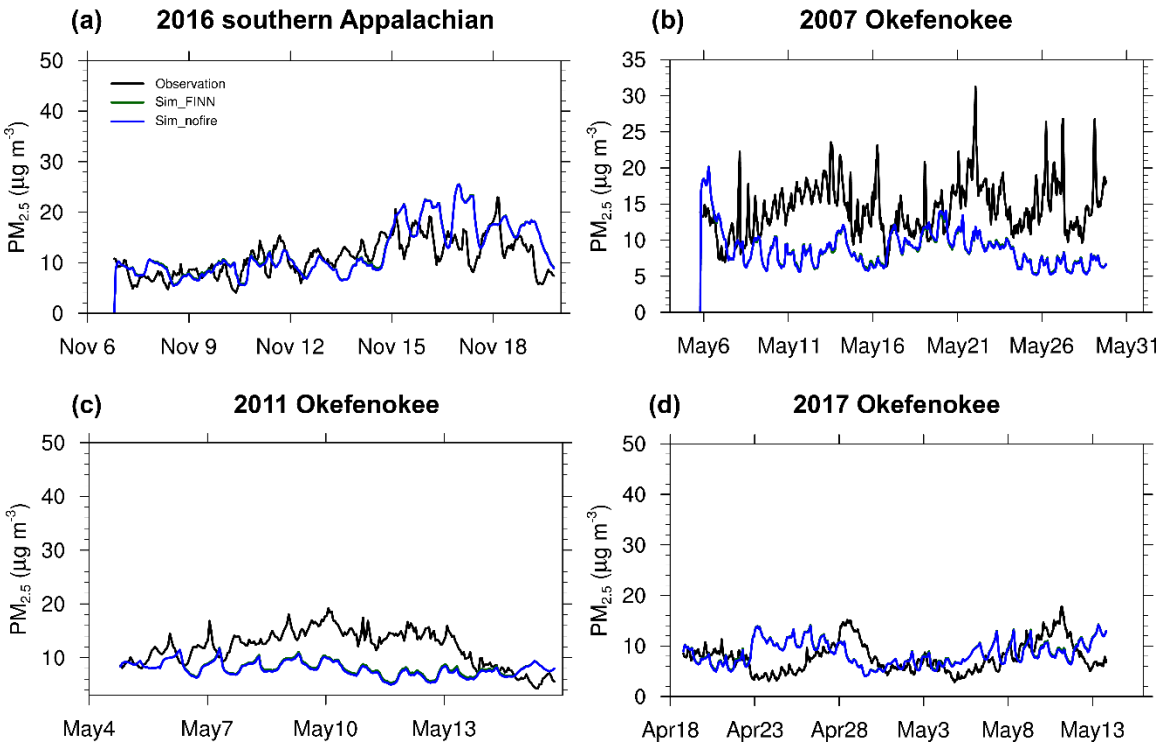

Figure S3. The time series of hourly surface PM2.5 concentrations averaged over the site and time that is not influenced by fire smoke ($PM_{2.5}$ concentration difference between Sim_FINN and Sim_nofire is less than 1 μg m^{-3}). Black: Measurements averaged over observation sites that is not influenced by fire smoke within the simulation domain. Green and blue: Simulations of Sim_FINN and Sim_nofire, respectively, averaged over the observation sites that is not influenced by fire smoke.

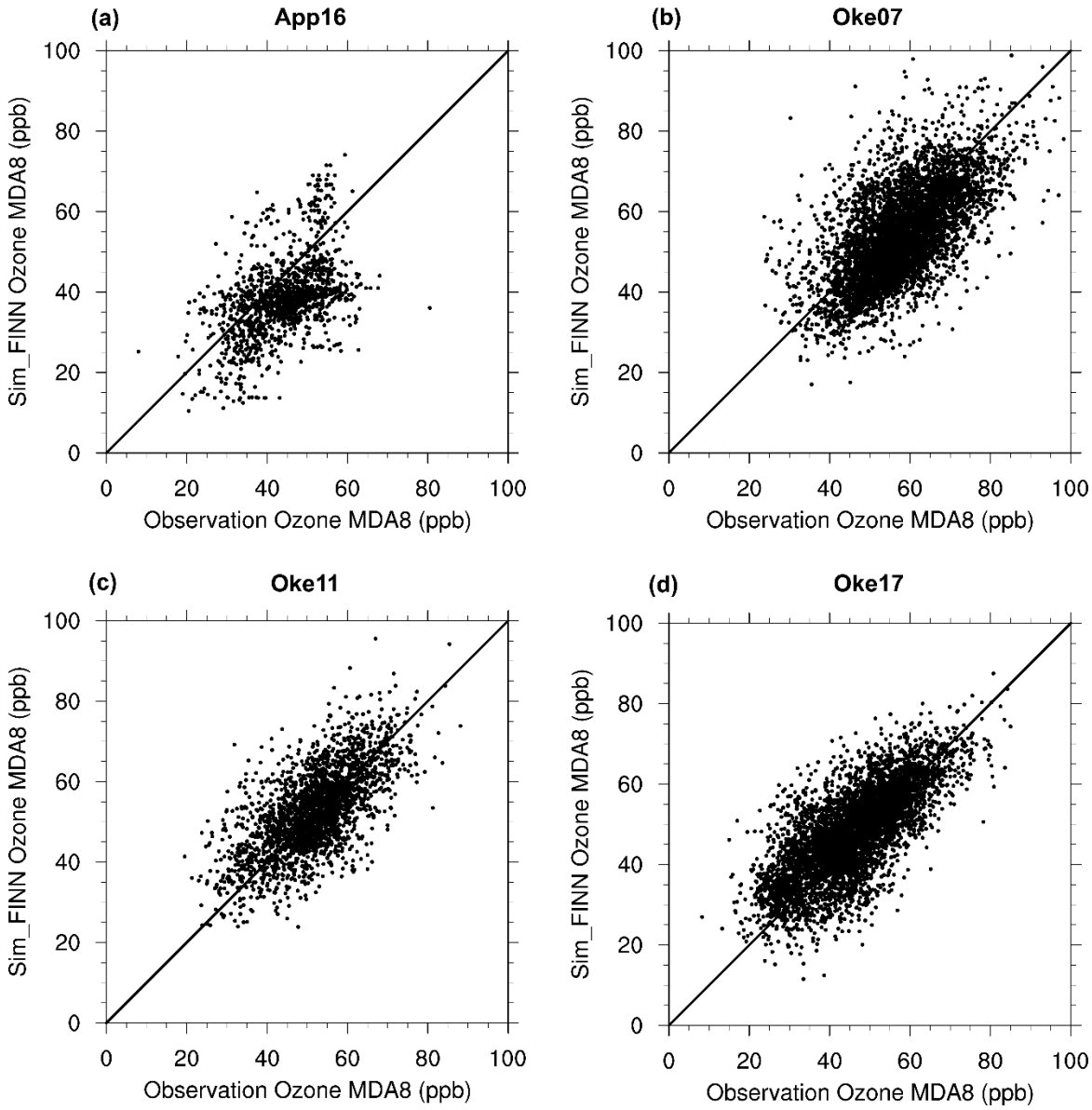

Figure S4. The comparison of MDA8 surface ozone concentrations between the observation and the baseline (sim_FINN) simulations.

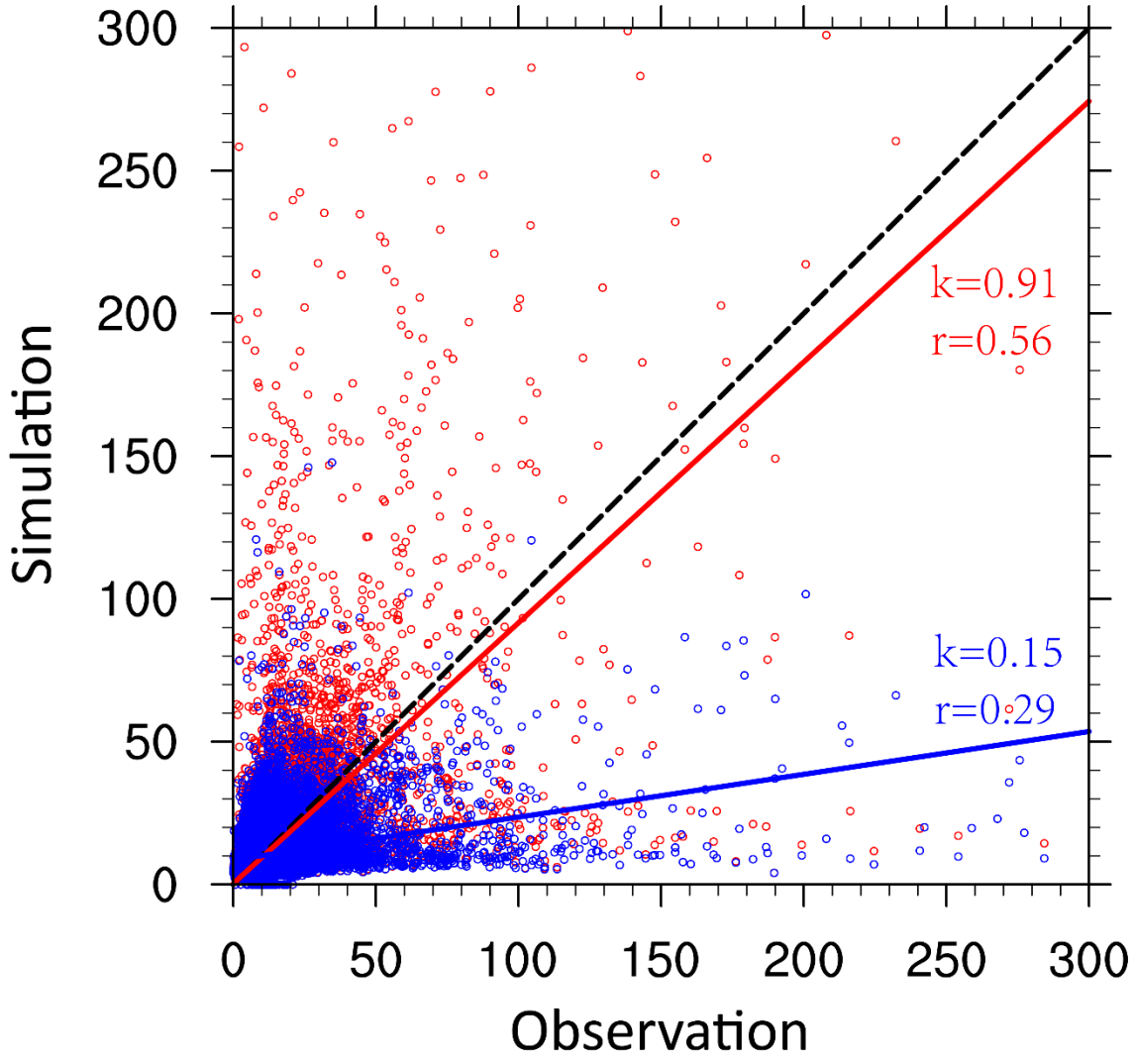

Figure S5. The comparison of Oke07 hourly surface $PM_{2.5}$ concentrations between the observation, the baseline (sim_FINN) simulations (blue), and the best (sim_FINN+duff) simulations (red), in unit of μg m^{-3}. The corresponding correlation coefficient (r) and the regression slope (k) is enclosed.

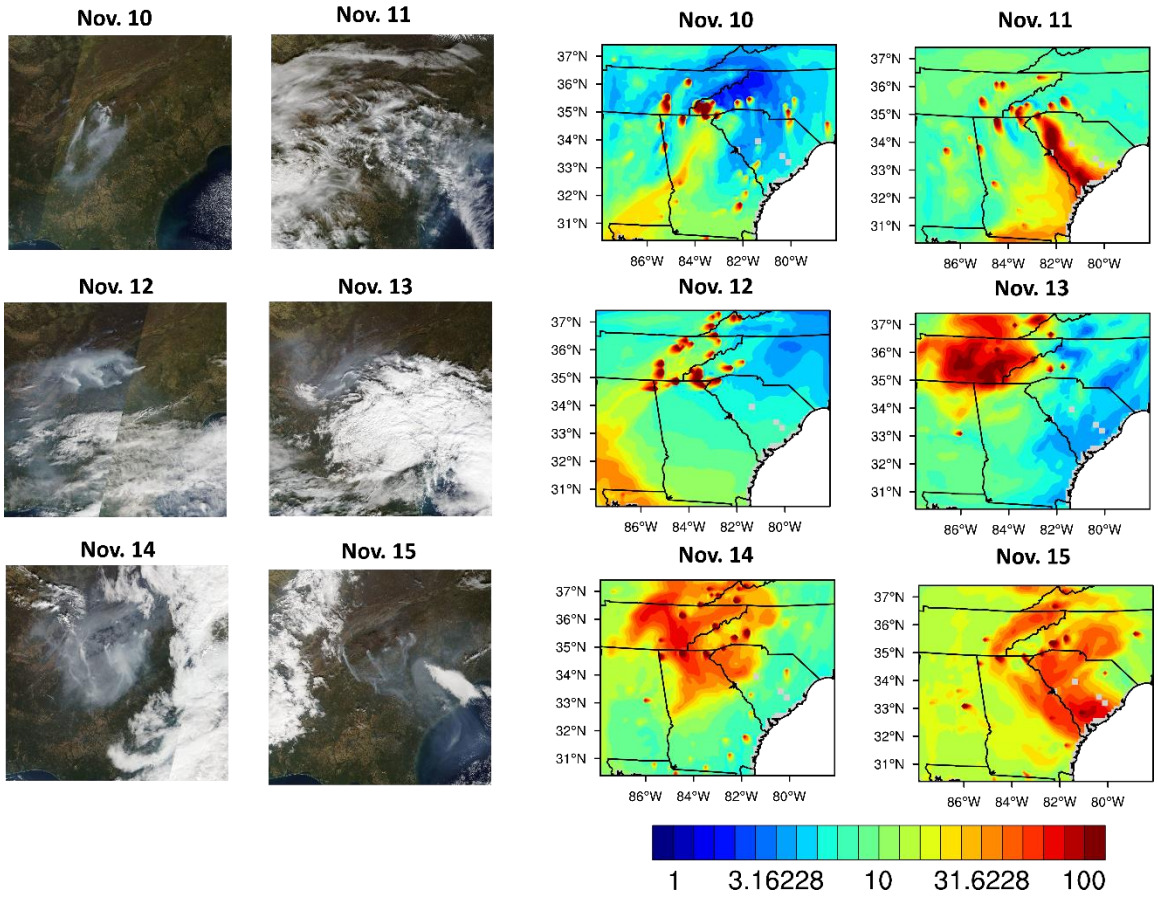

Figure S6. The MODIS Terra satellite image during November 10-15, 2016 over the APP16 fire compared with the corresponding surface $PM_{2.5}$ concentrations ($\mu g\ m^{-3}$) simulated in the sim_FINN+duff run at the hour of the satellite passing.

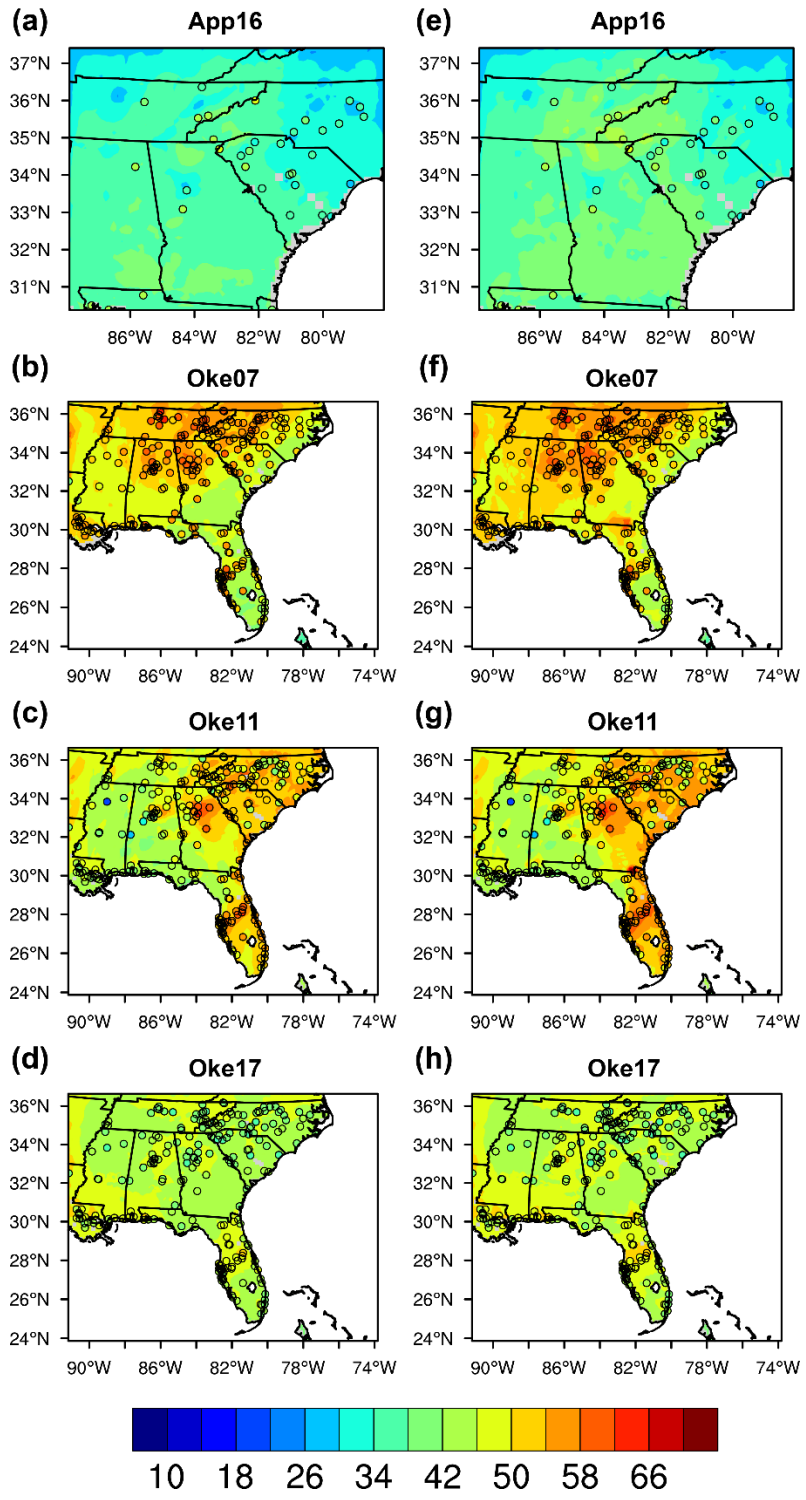

Figure S7. Mean day time (local time 10 am to 6 pm) ozone surface concentration (ppb). (a) App16 (November 7-19, 2016), (b) Oke07 (May 6-30, 2007), (c) Oke11 (May 6-15, 2011), and (d) Oke17 (April 19 to May 13, 2017) for sim_nofire. (e-h) are the corresponding fire cases for sim_FINN. The color scatters represent the observed mean day time surface ozone concentrations.

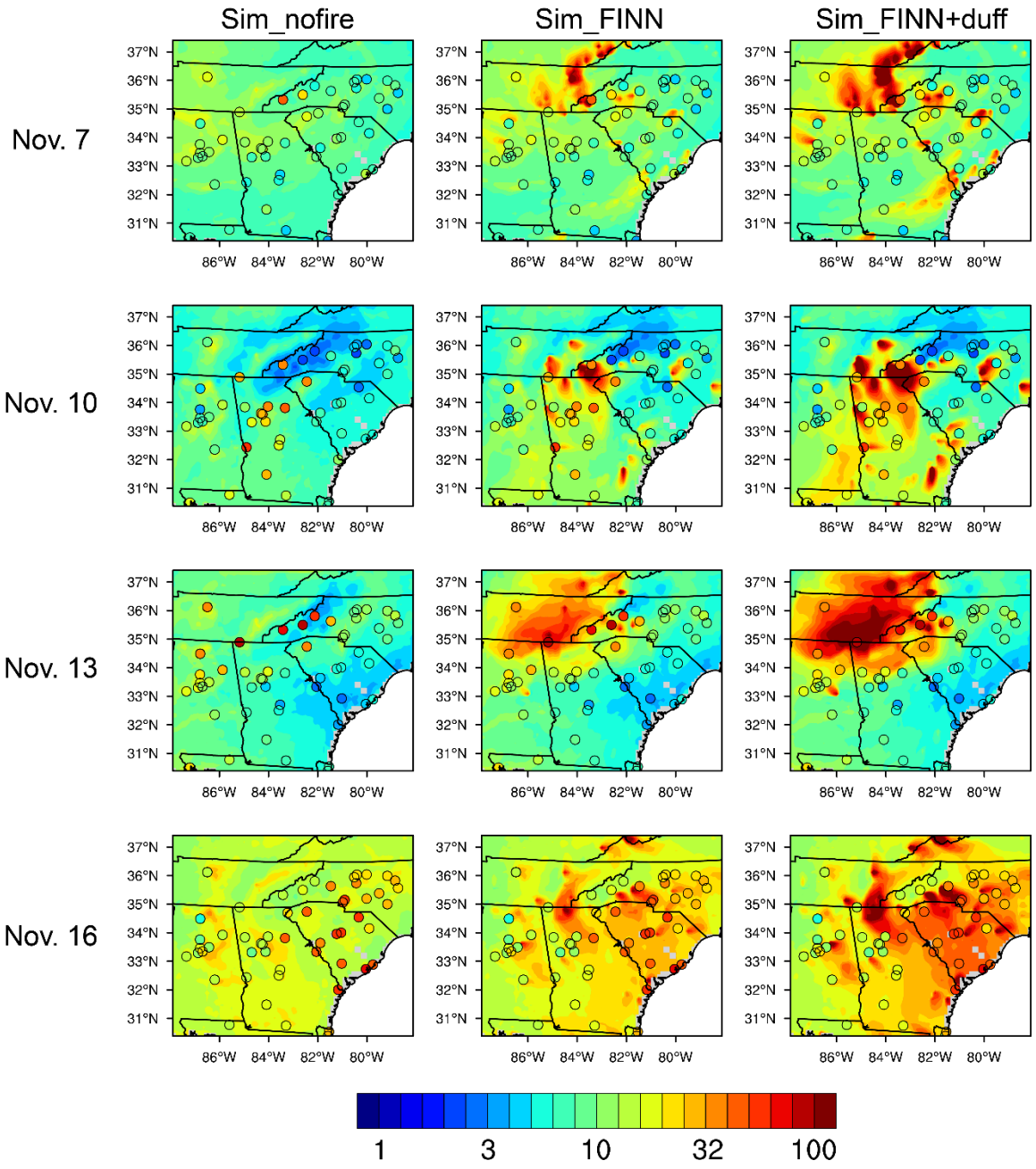

Figure S8. $PM_{2.5}$ daily mean surface concentration (μg m^{-3}) during App16 simulated in sim_nofire, sim_FINN and sim_FINN+duff runs. The colored scatters represent the corresponding observed $PM_{2.5}$ daily mean surface concentrations during the fire event.

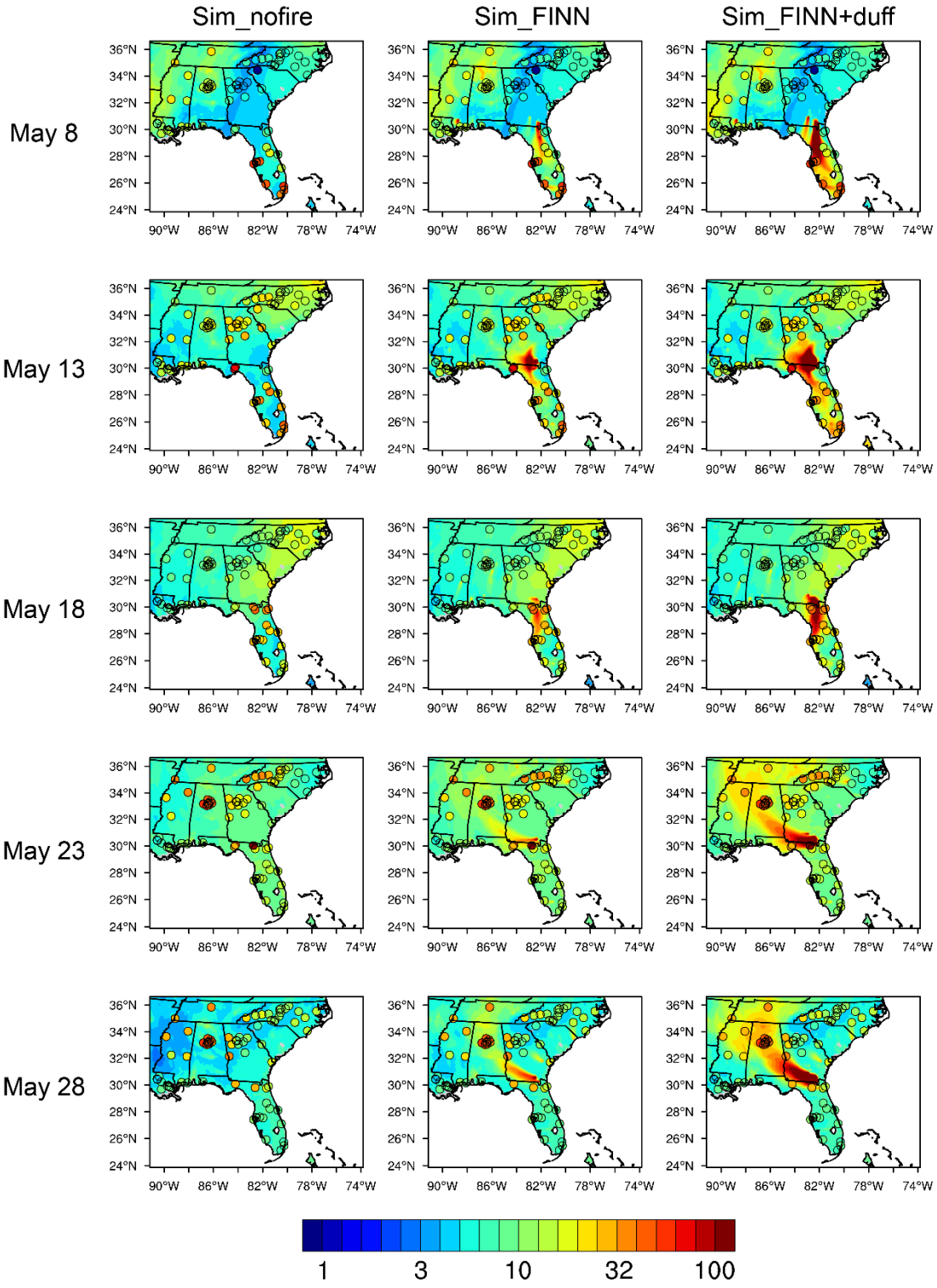

Figure S9. $PM_{2.5}$ daily mean surface concentration (μg m^{-3}) during Oke07 simulated in sim_nofire, sim_FINN and sim_FINN+duff runs. The colored scatters represent the corresponding observed $PM_{2.5}$ daily mean surface concentrations during the fire event.

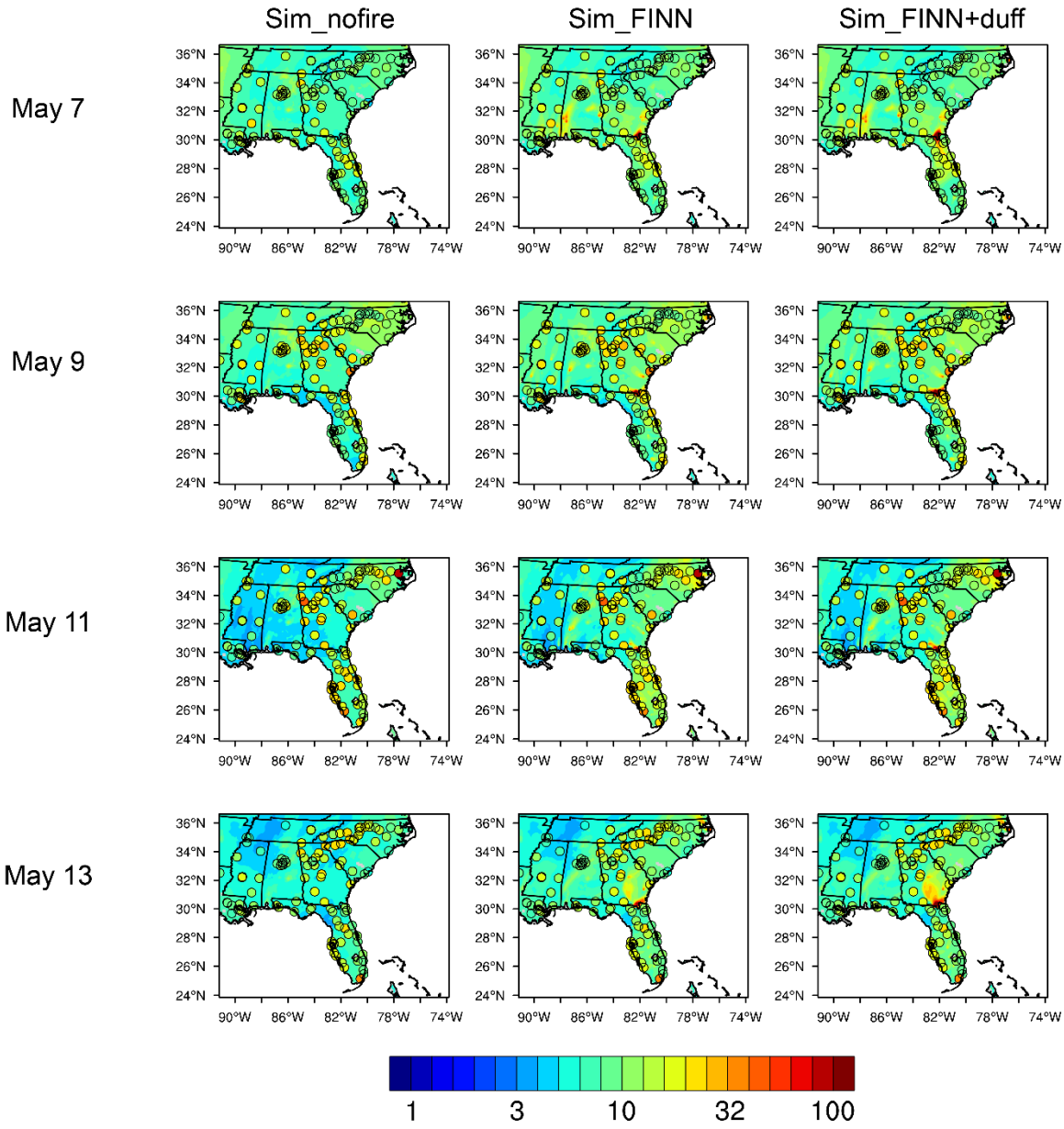

Figure S10. $PM_{2.5}$ daily mean surface concentration (μg m^{-3}) during Oke11 simulated in sim_nofire, sim_FINN and sim_FINN+duff runs. The colored scatters represent the corresponding observed $PM_{2.5}$ daily mean surface concentrations during the fire event.

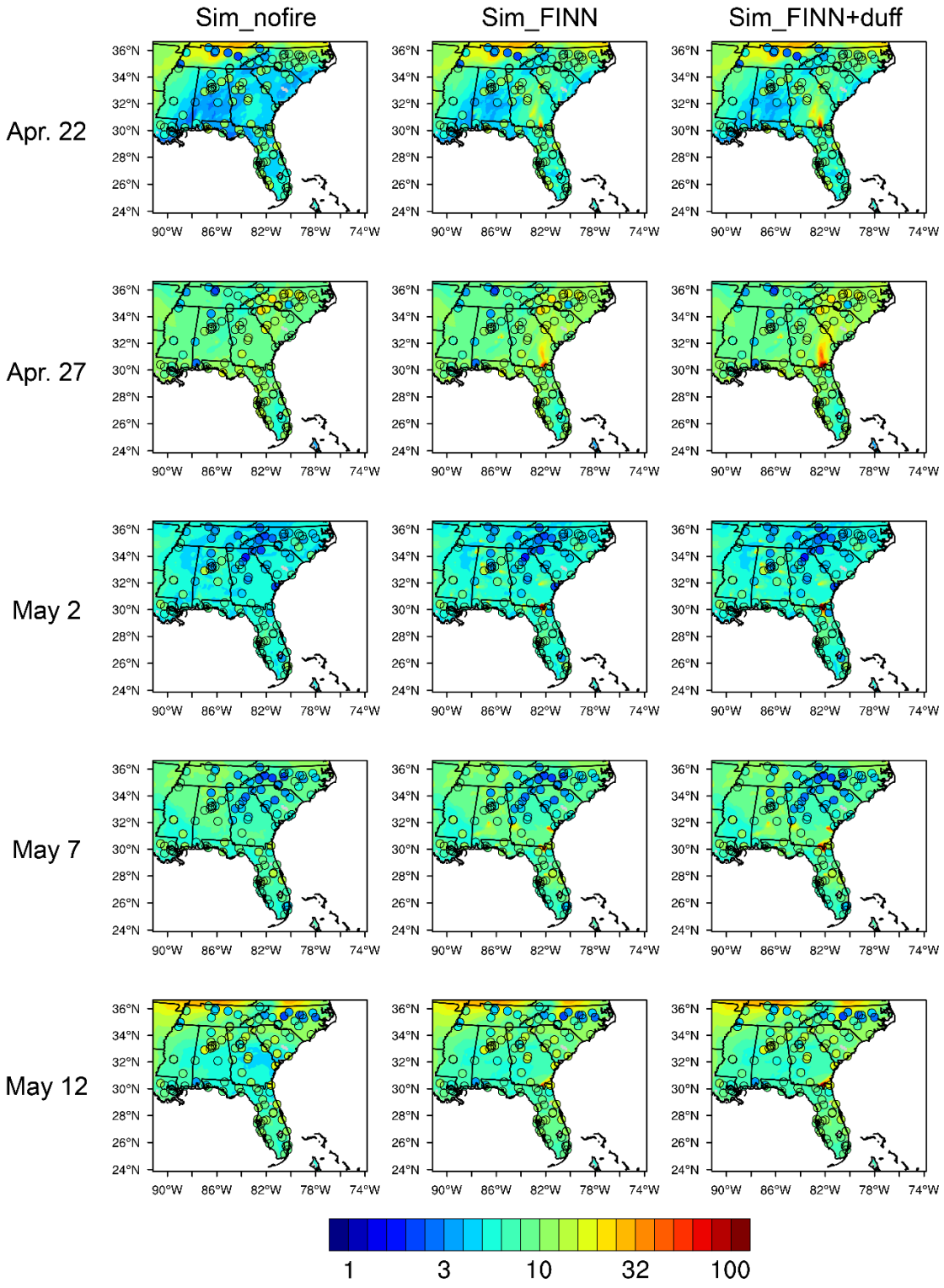

Figure S11. $PM_{2.5}$ daily mean surface concentration (μg m^{-3}) during Oke17 simulated in sim_nofire, sim_FINN and sim_FINN+duff runs. The colored scatters represent the corresponding observed $PM_{2.5}$ daily mean surface concentrations during the fire event.

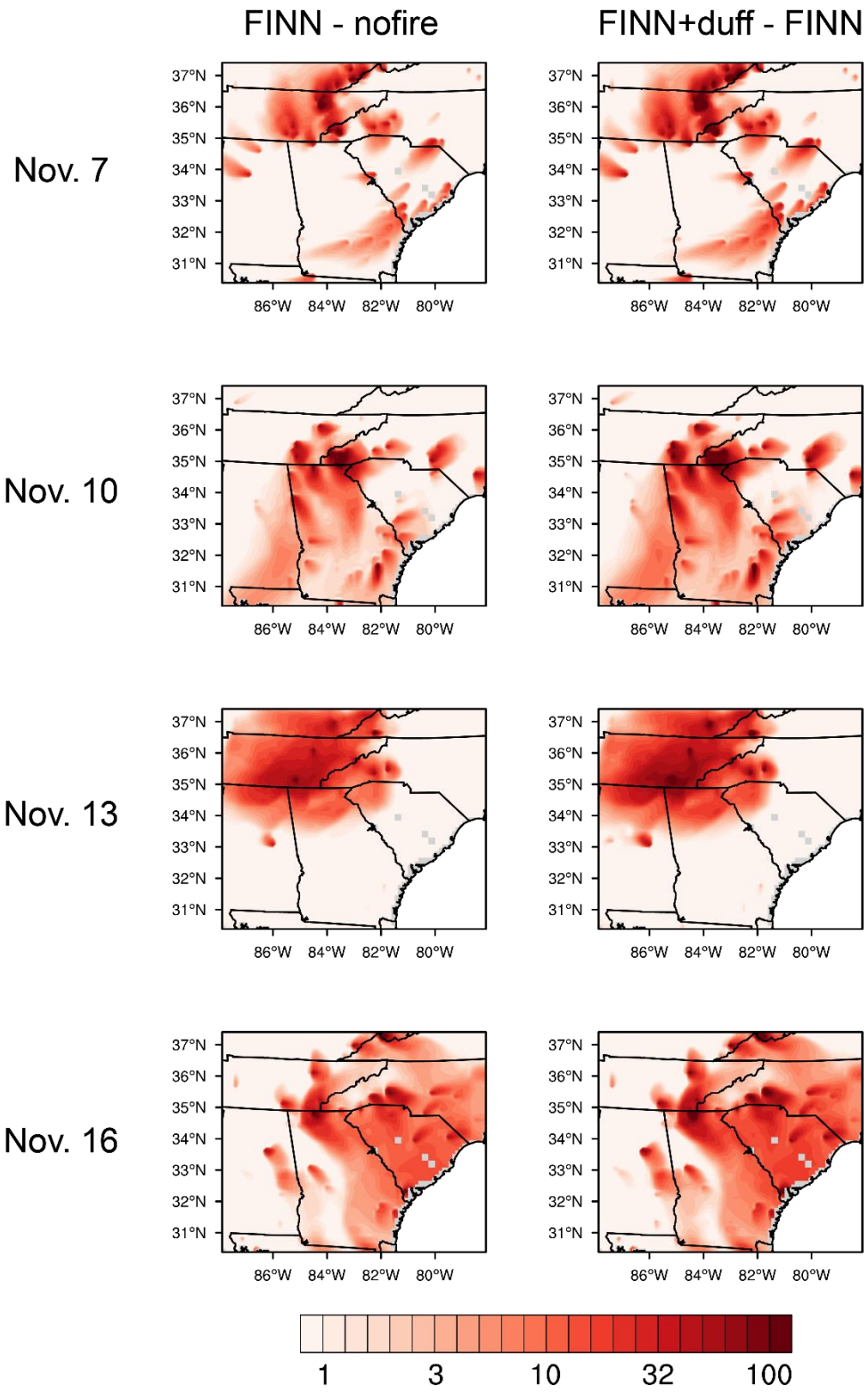

Figure S12. The $PM_{2.5}$ daily surface concentration differences (μg m^{-3}) between sim_FINN and sim_nofire and between sim_FINN+duff and sim_FINN during App16.

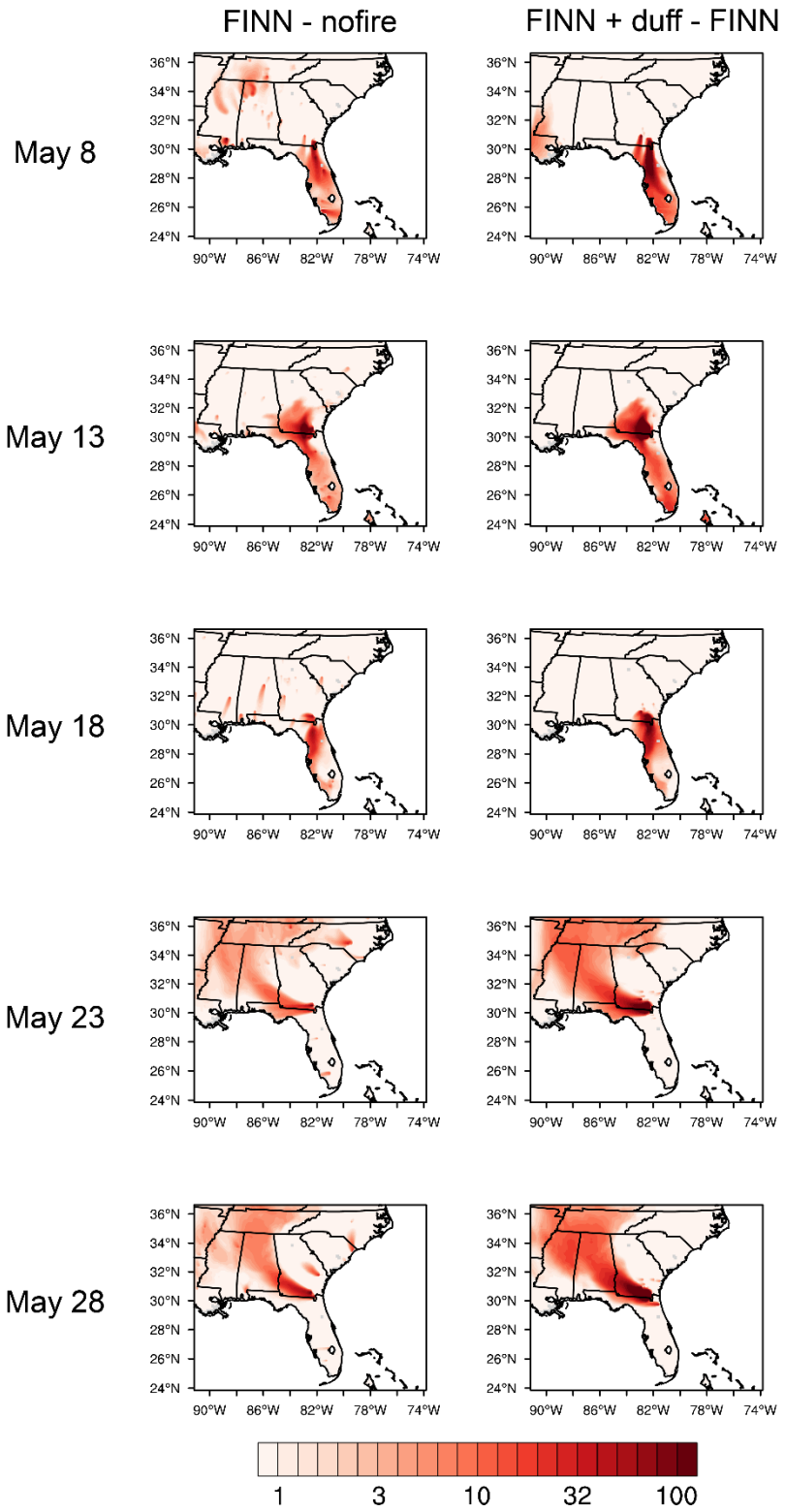

Figure S13. The $PM_{2.5}$ daily surface concentration differences (μg m^{-3}) between sim_FINN and sim_nofire and between sim_FINN+duff and sim_FINN during Oke07.

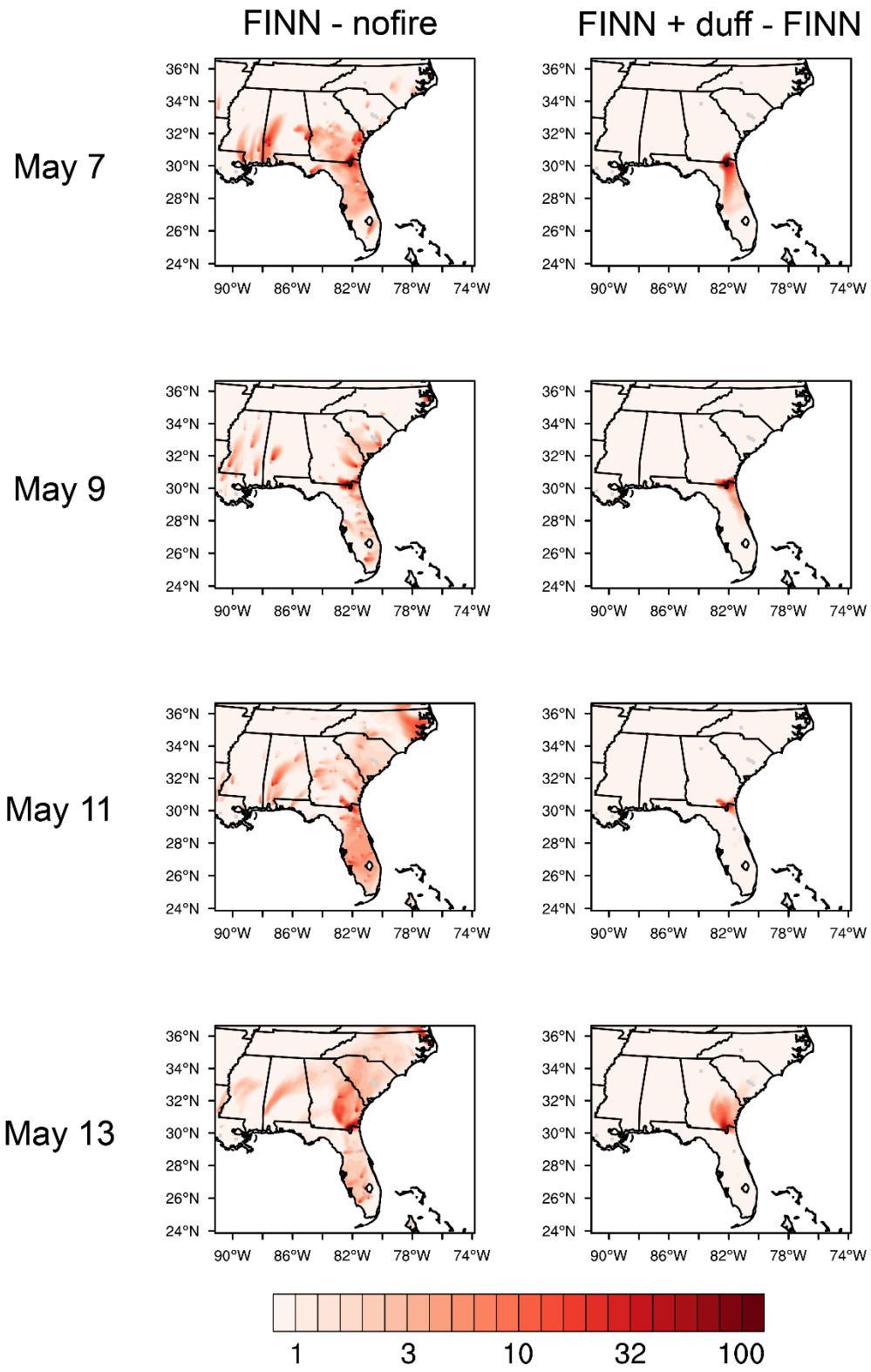

Figure S14. The $PM_{2.5}$ daily surface concentration differences (μg m^{-3}) between sim_FINN and sim_nofire and between sim_FINN+duff and sim_FINN during Oke11.

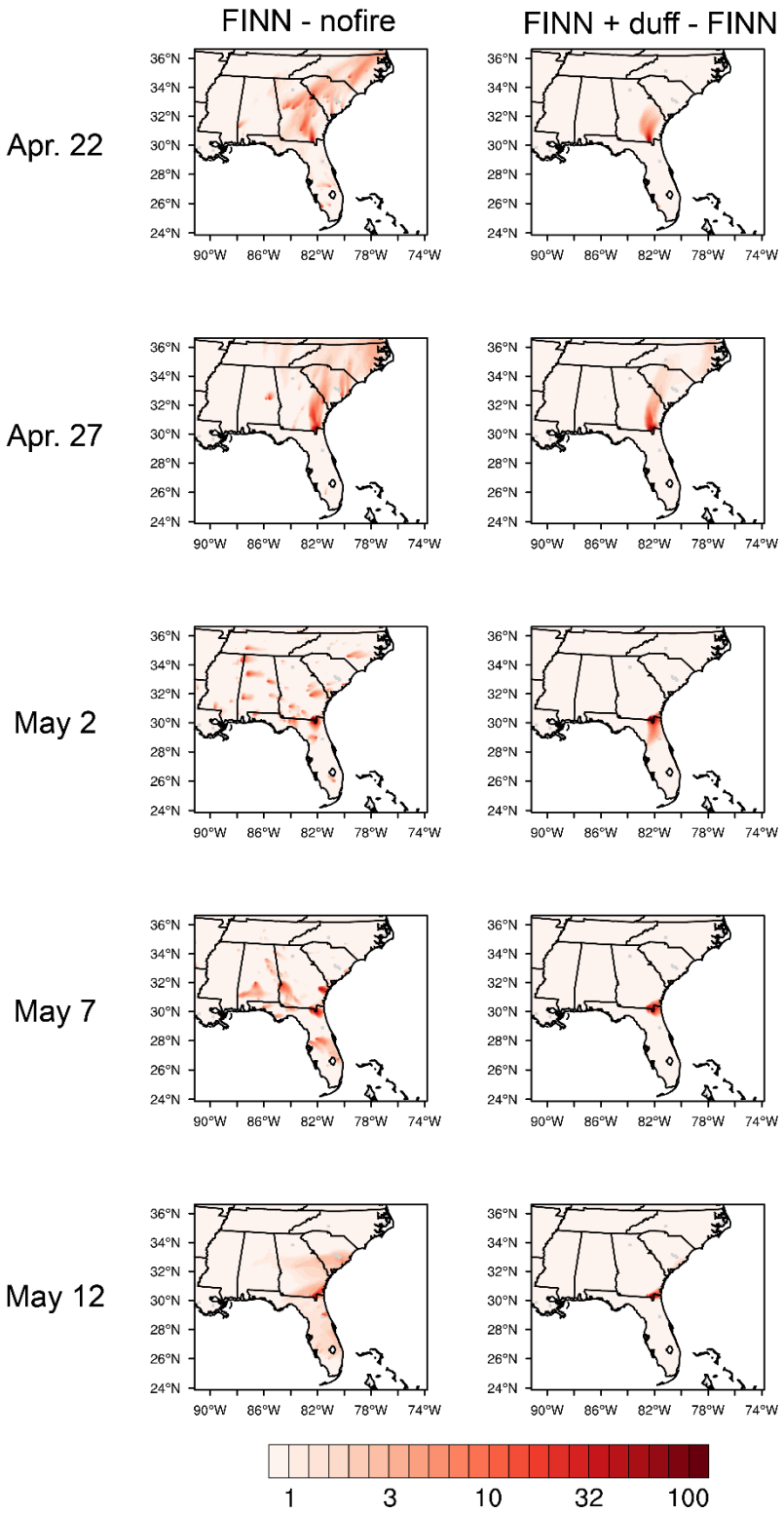

Figure S15. The $PM_{2.5}$ daily surface concentration differences (μg m^{-3}) between sim_FINN and sim_nofire and between sim_FINN+duff and sim_FINN during Oke17.

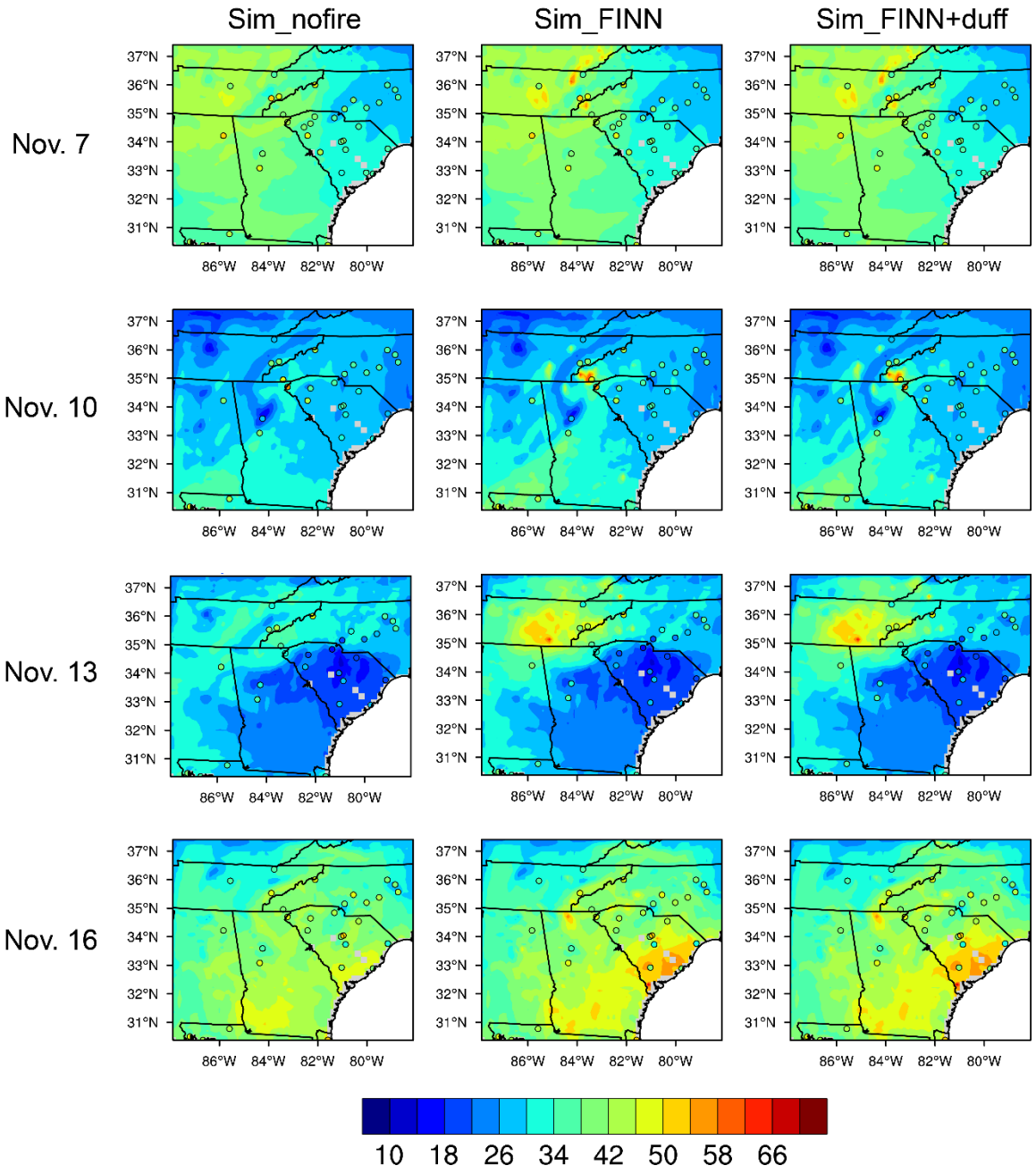

Figure S16. The ozone daytime surface concentration (averaged from local time 10 am to 6 pm; ppb.) during App16 simulated in sim_nofire, sim_FINN and sim_FINN+duff runs. The colored scatters represent the corresponding observed Ozone daytime surface concentrations during the fire event.

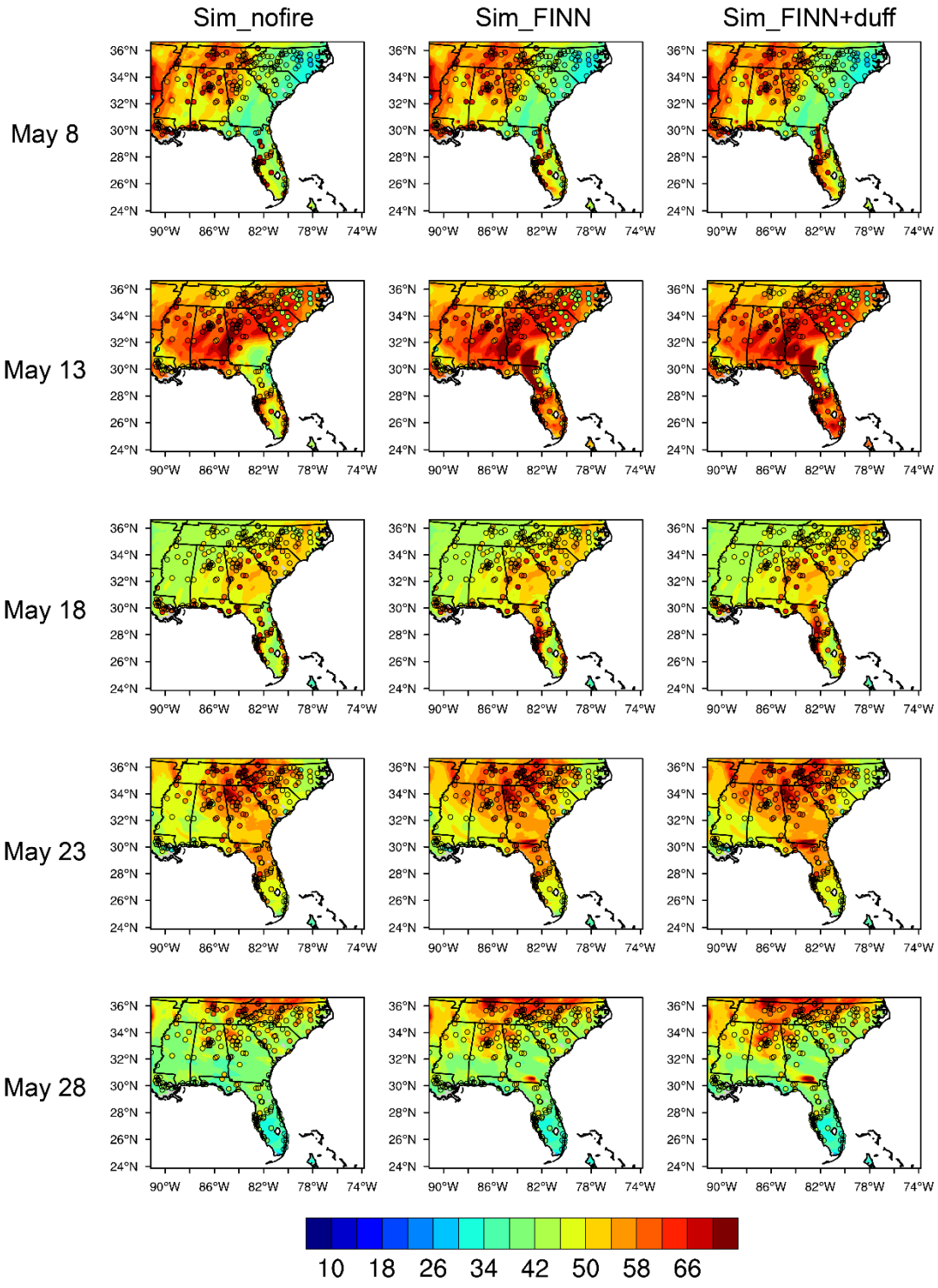

Figure S17. The ozone daytime surface concentration (averaged from local time 10 am to 6 pm; ppb.) during Oke07 simulated in sim_nofire, sim_FINN and sim_FINN+duff runs. The colored scatters represent the corresponding observed Ozone daytime surface concentrations during the fire event.

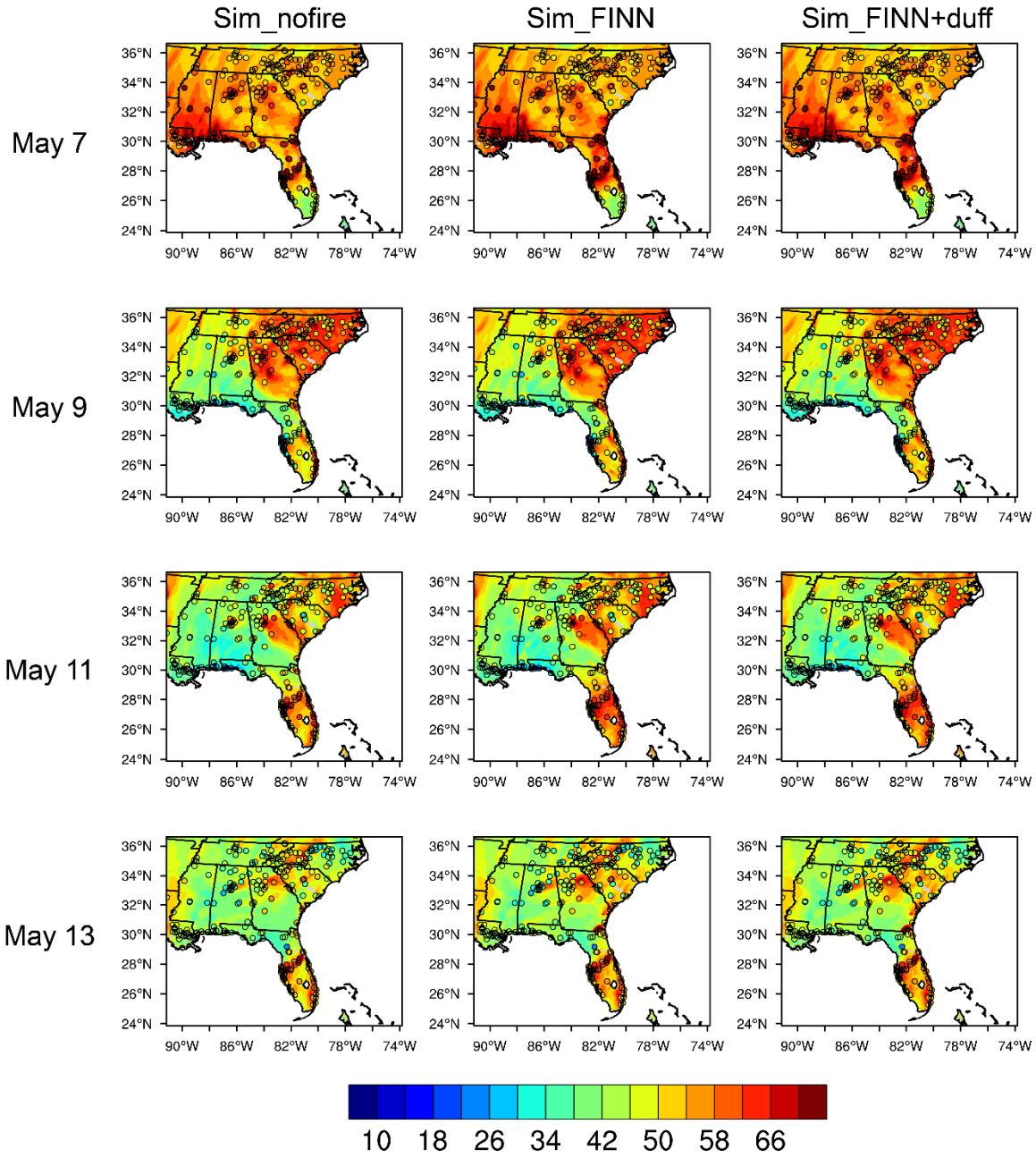

Figure S18. The ozone daytime surface concentration (averaged from local time 10 am to 6 pm; ppb.) during Oke11 simulated in sim_nofire, sim_FINN and sim_FINN+duff runs. The colored scatters represent the corresponding observed Ozone daytime surface concentrations during the fire event.

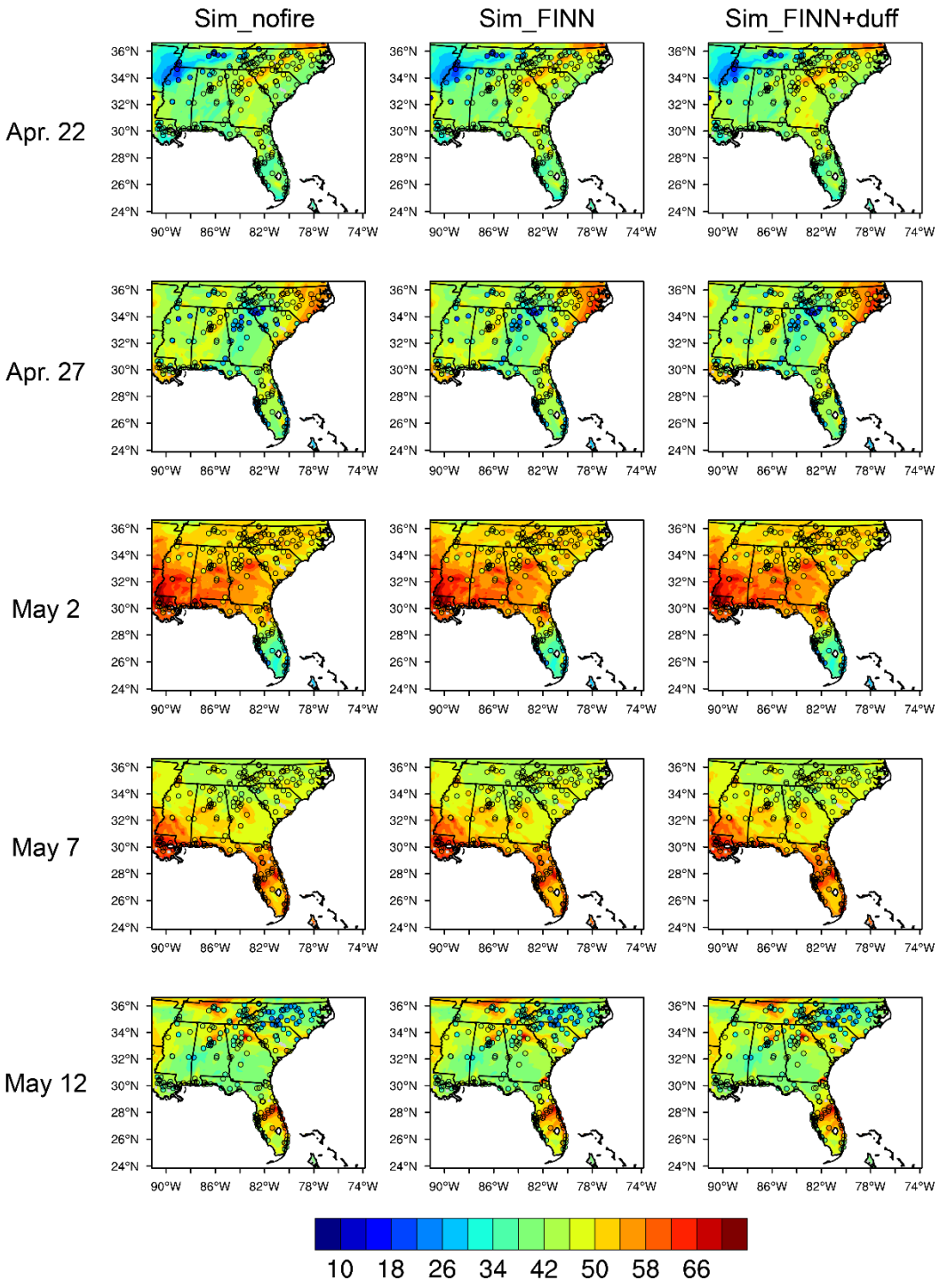

Figure S19. The ozone daytime surface concentration (averaged from local time 10 am to 6 pm; ppb.) during Oke17 simulated in sim_nofire, sim_FINN and sim_FINN+duff runs. The colored scatters represent the corresponding observed Ozone daytime surface concentrations during the fire event.

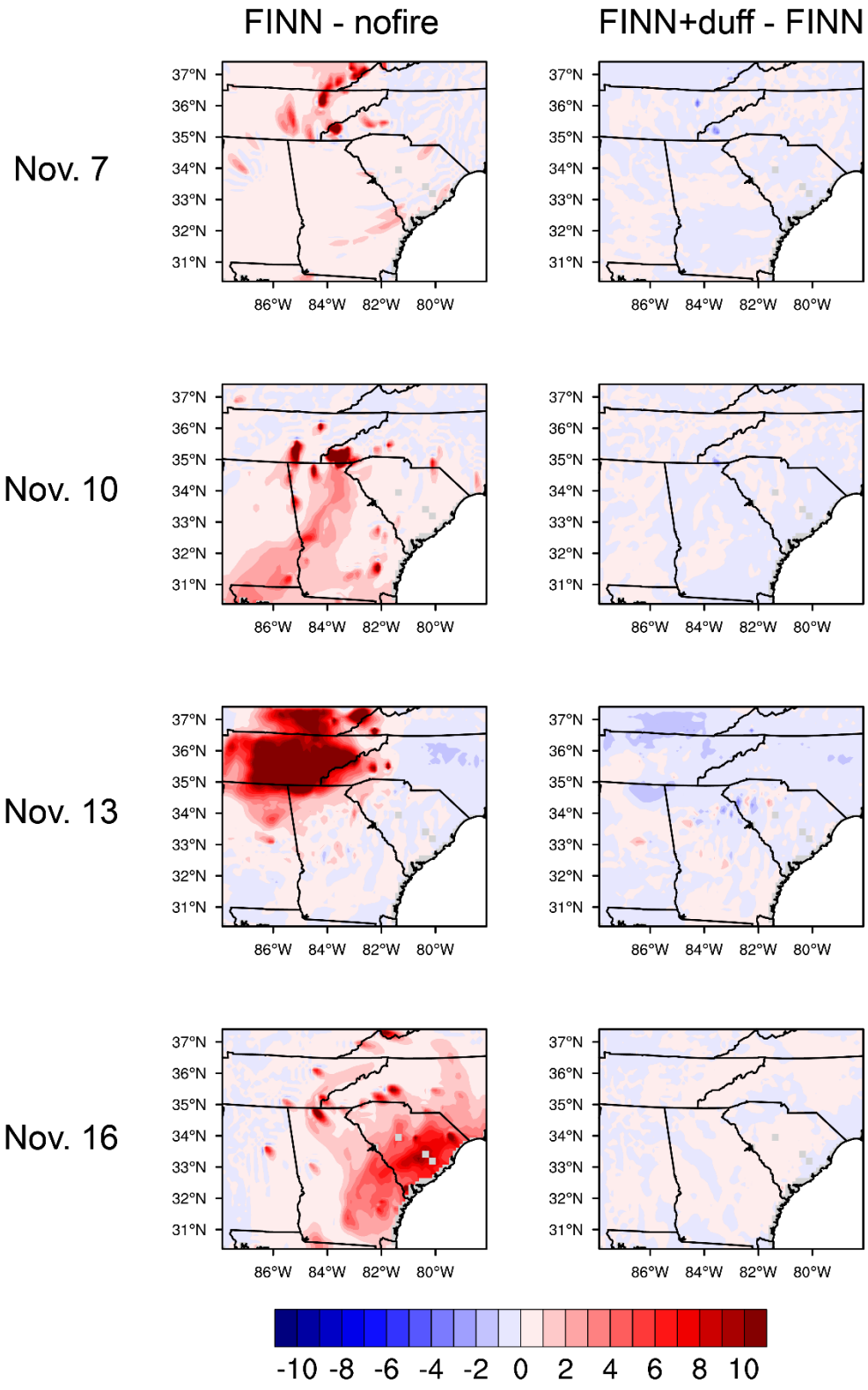

Figure S20. The ozone daytime surface concentration differences (ppb) between sim_FINN and sim_nofire and between sim_FINN+duff and sim_FINN during App16.

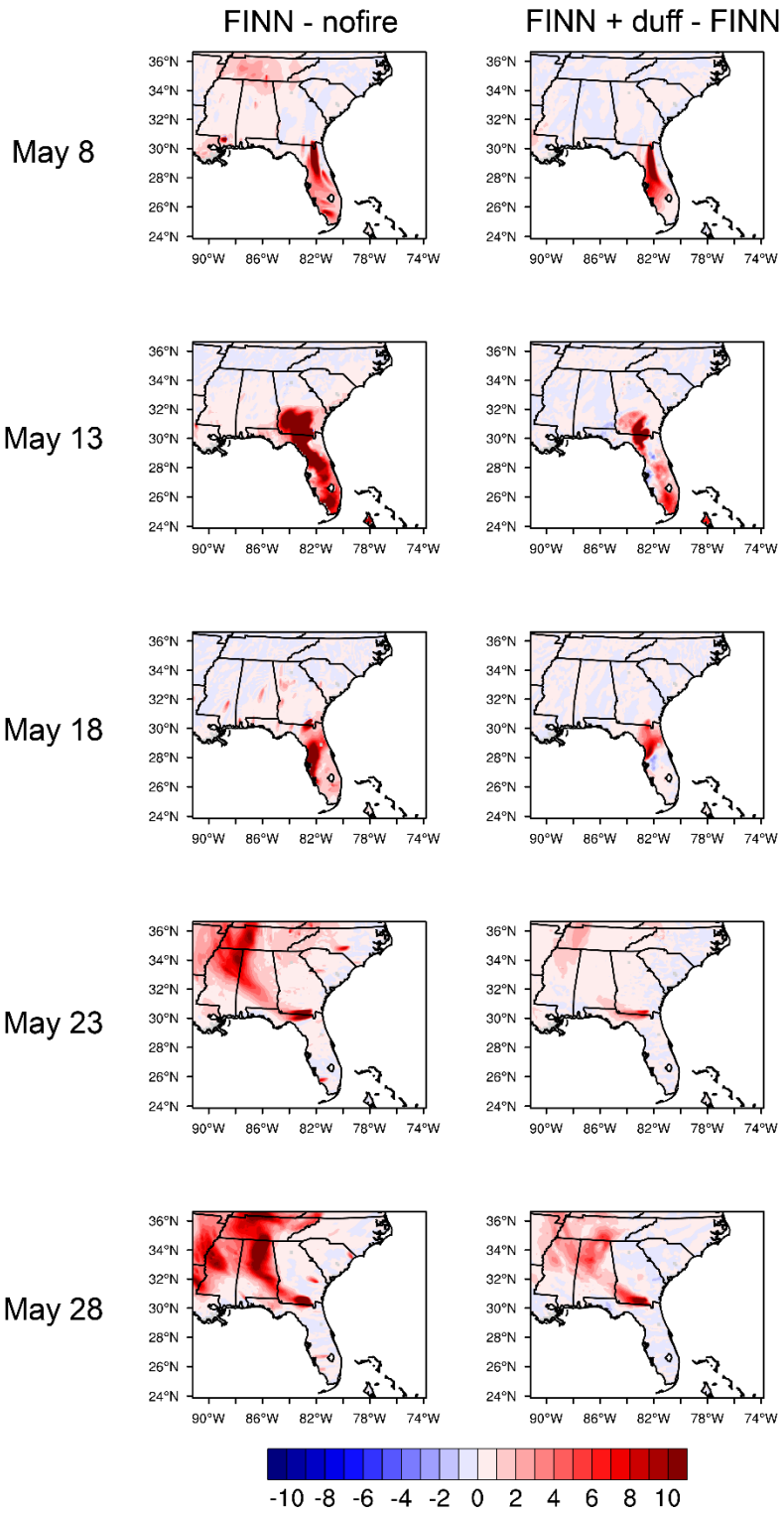

Figure S21. The ozone daytime surface concentration differences (ppb) between sim_FINN and sim_nofire and between sim_FINN+duff and sim_FINN during Oke07.

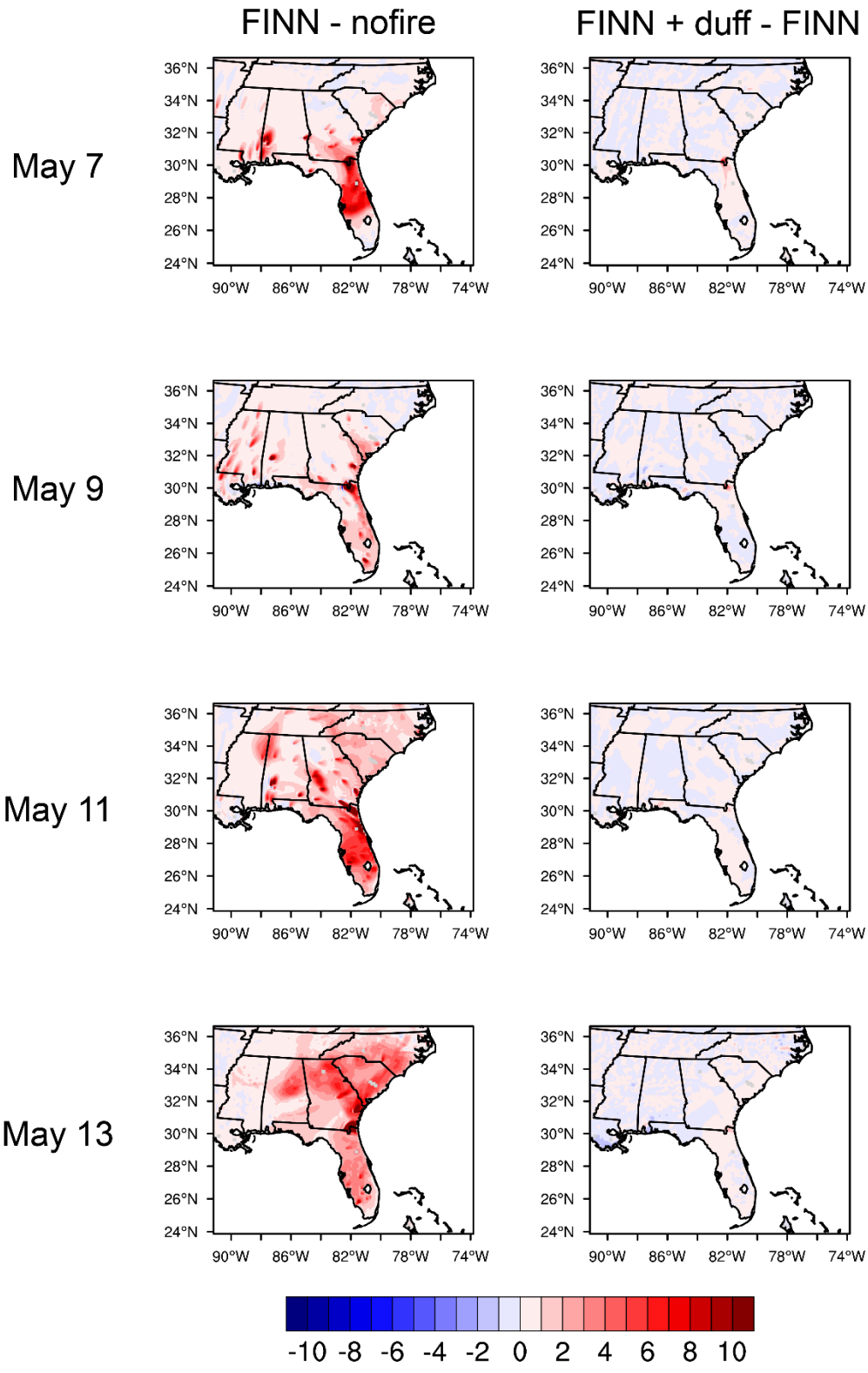

Figure S22. The ozone daytime surface concentration differences (ppb) between sim_FINN and sim_nofire and between sim_FINN+duff and sim_FINN during Oke11.

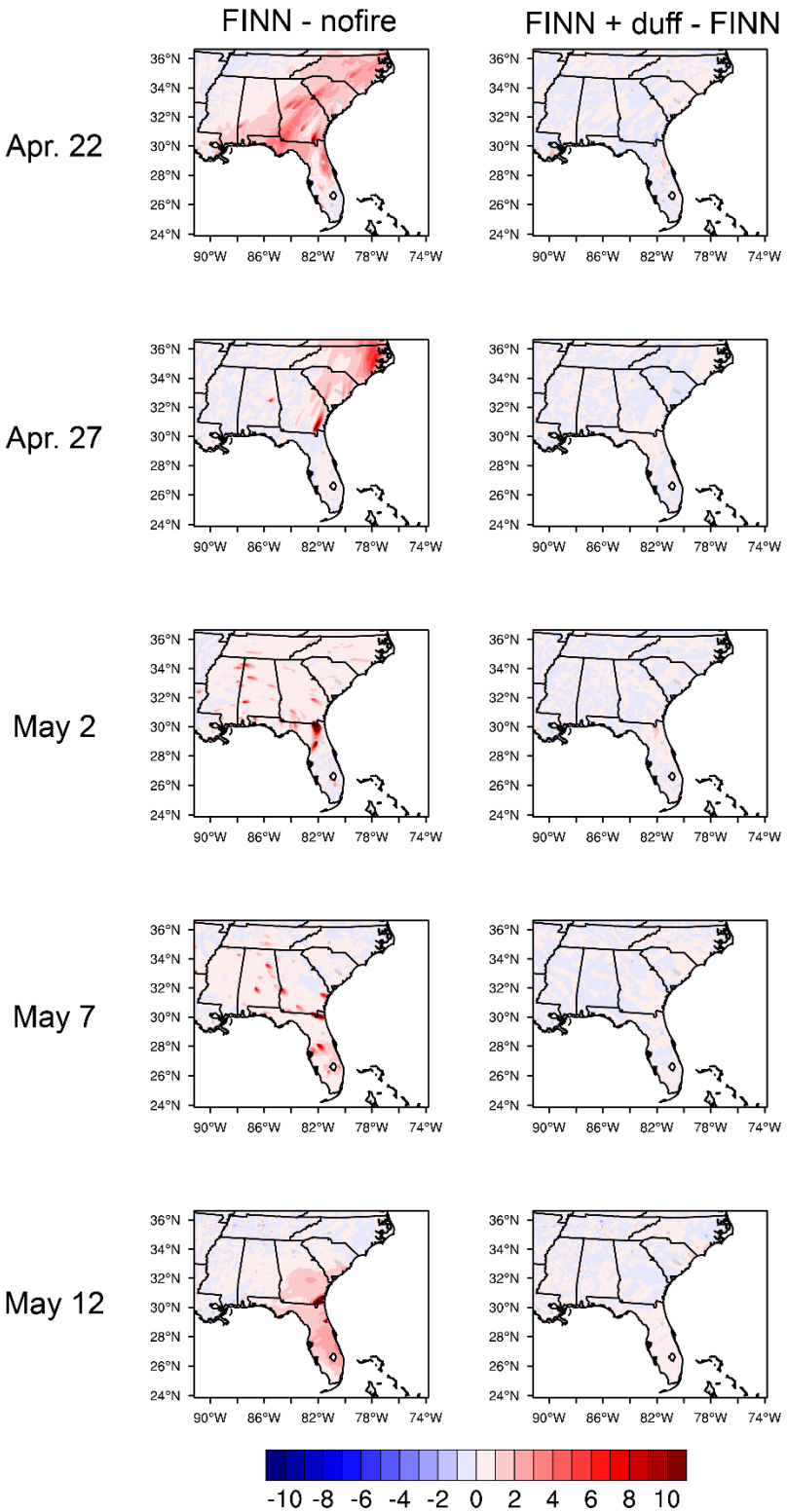

Figure S23. The ozone daytime surface concentration differences (ppb) between sim_FINN and sim_nofire and between sim_FINN+duff and sim_FINN during Oke17

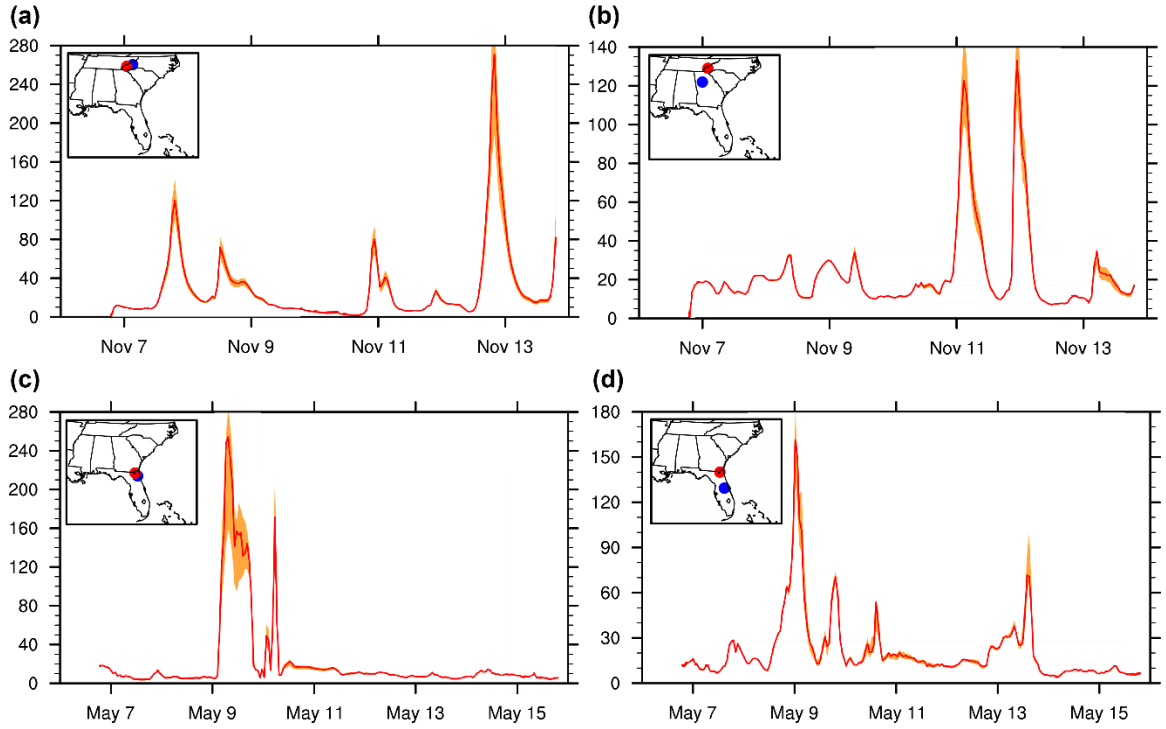

Figure S24. The time series of hourly surface $PM_{2.5}$ (μg m^{-3}) concentrations in the sim_FINN+duff simulations. (a, b) App16. (c, d) Oke07. The shaded red represents the $PM_{2.5}$ variation from the sensitivity runs changing the duff emission by ± 30%. The fire location (red) and site location (blue) are shown in the map attached to each panel. The studied sites are located in (a) Buncombe county, North Carolina, (b) Fulton county, Georgia, (c) Duval county, Florida and (d) Orange county, Florida.

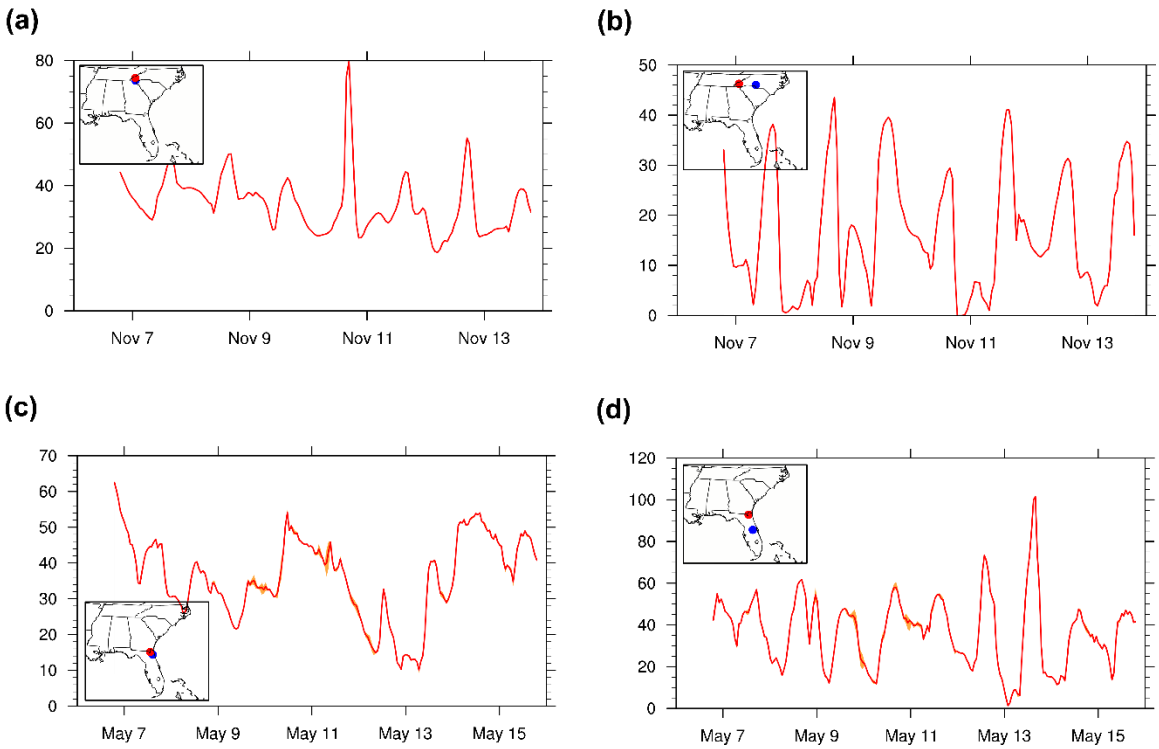

Figure S25. The time series of hourly surface ozone (ppb) concentrations in the sim_FINN+duff simulations. (a, b) App16. (c, d) Oke07. The shaded red represents the $PM_{2.5}$ variation from the sensitivity runs changing the duff emission by ± 30%. The fire location (red) and site location (blue) are shown in the map attached to each panel. The studied sites are located in (a) Macon county, North Carolina, (b) Fulton county, Georgia, (c) Duval county, Florida and (d) Orange county, Florida.

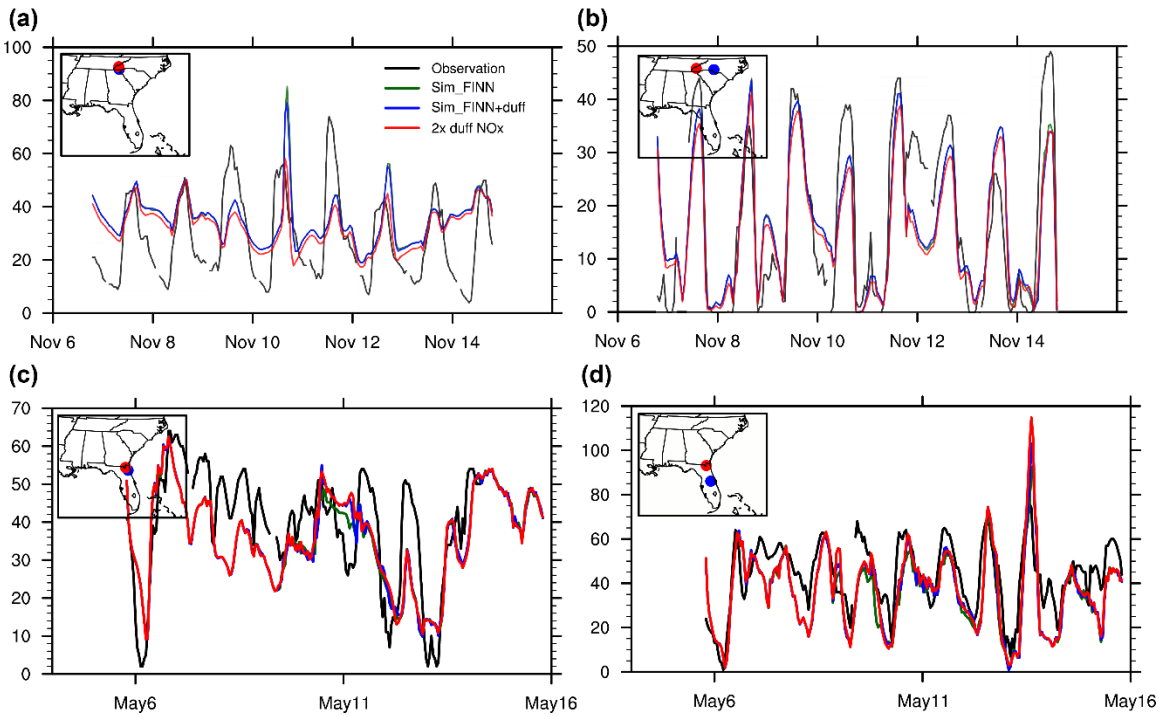

Figure S26. Comparisons of in-situ hourly surface ozone concentrations (ppb) among the observation (black), sim_FINN (green), sim_FINN+duff (blue) and 2x duff NOx simulations. (a, b) App16. (c, d) Oke07. The fire location (red) and site location (blue) are shown in the map attached to each panel. The studied sites are located in (a) Macon county, North Carolina, (b) Fulton county, Georgia, (c) Duval county, Florida and (d) Orange county, Florida.

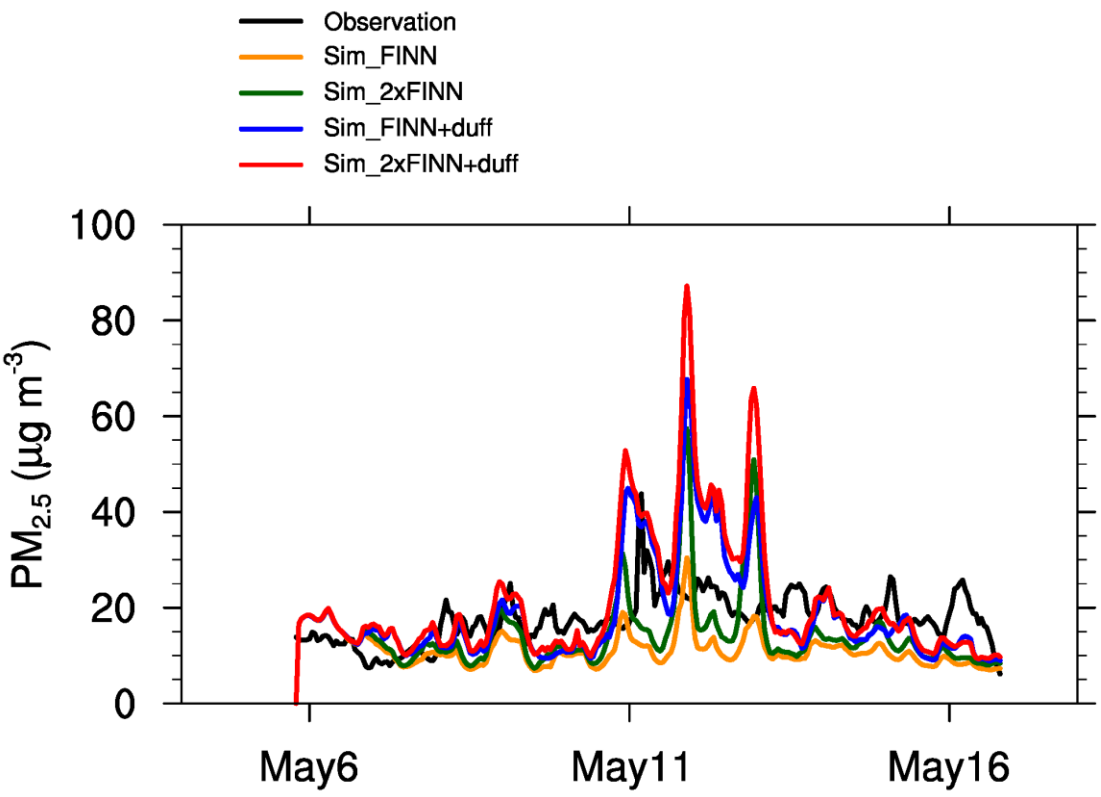

Figure S27. The time series of hourly surface $PM_{2.5}$ concentrations from May 6 – 16, 2017 in the observations, sim_FINN, sim_FINN+duff, and corresponding simulations with FINN emission doubled (sim_2xFINN and sim_2xFINN+duff) in the simulated region.

Table S1. Summary of previous studies of the PM emission factors of duff/peat/organic soil burnings.

Source	Region	Fuel type	Emission Factor (g/kg)	Note
Geron and Hays (2013)	Southeastern US	Peat/Organic soil	34 - 79	34-79 g/kg for ground fire; 9-16 g/kg for prescribed fire
Black et al. (2016)	Southeastern US	Peat	7.1 and 5.9	
Benner (1977)	Southeastern US	Peat/Organic soil	44 ± 9	Total suspended particulate (TSP) is measured.
McMahon et al. (1980)	Southeastern US	Peat	30 ± 20	
Urbanski (2014)	US	Duff/Organic soil	50 ± 16	Average of ground fire values by Geron and Hays (2013)
Yokelson et al. (2013)	US	Organic soil	20	prescribed burning
Kiely et al. (2020)	Equatorial Asia	Peat	22.3	Summarized from previous studies, used in model simulations
Roulston et al. (2018)	Southeast Asia	Peat	8 - 58	Average 24 g/kg; newly ignited fire has higher emission factor.
Jayarathne et al. (2018)	Indonesia	Peat	17	
Stockwell et al. (2016)	Indonesia	Peat	15.7-29.6	
May et al. (2014)	Indonesia	Peat	34.9	PM1 emission factor from lab burns
Bertschi et al. (2003)	Africa	Duff	6 - 16	
Andreae (2019)	Global	Peat	18.9 ± 2.3	Summarized from previous studies
Akagi et al. (2011)	Global	Peat	9.92	Summarized from previous studies
Giglio et al. (2013)	Global	Peat	9.1	Used in GFED4

Table S2. Summary of the duff burning emission factors of the gas phase species used in this study, based on Yokelson et al. (2013)

Species	Emission factor (g/kg)	Species	Emission factor (g/kg)
CO	271	CH_3OH	3.24
NO	0.559	MEK	0.422
SO_2	1.76	Toluene	2.5965
NMOC	68.67	NH_3	2.67
Bigalk	0.658	NO_2	0.176
Bigene	1.4332	Open	1.1998
C_2H_4	1.43	$C_{10}H_{16}$	1.1102
C_2H_5OH	0.495	CH_3COOH	7.47
C_2H_6	1.339	MGLY	0.153
C_3H_8	0.797	Acetol	0.277
C_3H_6	1.22	Isoprene	0.0786
CH_2O	1.88	MACK	0.102
CH_{3CHO}	2.7	MVK	0.421
CH_3COCH_3	1.39	CH_4	7.47

Table S3. Summary of previous studies of the NO_x emission factors of duff burnings.

Source	NO emission factor (g/kg)		NO2 emission factor (g/kg)	
	duff	above-ground fuel	duff	above-ground fuel
Burling et al. (2010)	0.738	1.720 ± 0.454	0.232	1.023 ± 0.286
Selimovic et al. (2018)	0.56-0.93	1.78(0.44-3.53)	0.77-1.30	1.26(0.44-7.04)
McMeeking et al. (2009)	2.0 ± 0.7	1.7-4.6	1.0 ± 0.5	0.3-1.6
Clements and McMahon (1980)	11.58	0.23-16.50	2.7	0.06-7.32
Yokelson et al. (2013)	0.559*	0.77-1.74	0.176*	1.01-2.68

* The number is used in this study.

Table S4 Summary of duff flaming rate and the corresponding fuel loading for the studied fire cases.

Fire case	mean duff flaming depth and rate (cm/day)	duff fuel loading (kg/m2)
App16	4.6	3.15
Oke07	4.6	3.15
Oke11	0.95	0.65
Oke17	1.68	1.15
ER08	4.6	3.15
PB11	4.6	3.15

REFERENCES

Akagi, S., Yokelson, R. J., Wiedinmyer, C., Alvarado, M., Reid, J., Karl, T., Crounse, J., and Wennberg, P.: Emission factors for open and domestic biomass burning for use in atmospheric models, Atmospheric Chemistry and Physics, 11, 4039-4072, https://doi.org/10.5194/acp-11-4039-2011, 2011.

Andreae, M. O.: Emission of trace gases and aerosols from biomass burning–an updated assessment, Atmospheric Chemistry and Physics, 19, 8523-8546, https://doi.org/10.5194/acp-19-8523-2019, 2019.

Benner, W. H.: Photochemical reactions of forest fire combustion products, University of Florida, 1977.

Bertschi, I., Yokelson, R. J., Ward, D. E., Babbitt, R. E., Susott, R. A., Goode, J. G., and Hao, W. M.: Trace gas and particle emissions from fires in large diameter and belowground biomass fuels, Journal of Geophysical Research: Atmospheres, 108, 2003.

Black, R. R., Aurell, J., Holder, A., George, I. J., Gullett, B. K., Hays, M. D., Geron, C. D., and Tabor, D.: Characterization of gas and particle emissions from laboratory burns of peat, Atmospheric Environment, 132, 49-57, 2016.

Geron, C., and Hays, M.: Air emissions from organic soil burning on the coastal plain of North Carolina, Atmospheric environment, 64, 192-199, https://doi.org/10.1016/j.atmosenv.2012.09.065, 2013.

Giglio, L., Randerson, J. T., and Werf, G. R.: Analysis of daily, monthly, and annual burned area using the fourth-generation global fire emissions database (GFED4), Journal of Geophysical Research: Biogeosciences, 118, 317-328, https://doi.org/10.1002/jgrg.20042, 2013.

Jayarathne, T., Stockwell, C. E., Gilbert, A. A., Daugherty, K., Cochrane, M. A., Ryan, K. C., Putra, E. I., Saharjo, B. H., Nurhayati, A. D., and Albar, I.: Chemical characterization of fine particulate matter emitted by peat fires in Central Kalimantan, Indonesia, during the 2015 El Niño, Atmospheric Chemistry and Physics, 18, 2585-2600, 2018.

Kiely, L., Spracklen, D. V., Wiedinmyer, C., Conibear, L. A., Reddington, C. L., Arnold, S. R., Knote, C., Khan, M. F., Latif, M. T., and Syaufina, L.: Air quality and health impacts of vegetation and peat fires in Equatorial Asia during 2004–2015, Environmental Research Letters, https://doi.org/10.1088/1748-9326/ab9a6c, 2020.

May, A., McMeeking, G., Lee, T., Taylor, J., Craven, J., Burling, I., Sullivan, A., Akagi, S., Collett Jr, J., and Flynn, M.: Aerosol emissions from prescribed fires in the United States: A synthesis of laboratory and aircraft measurements, Journal of Geophysical Research: Atmospheres, 119, 11,826-811,849, 2014.

McMahon, C. K., Wade, D. D., and Tsoukalas, S. N.: Combustion characteristics and emissions from burning organic soils, In: 73rd Annual Meeting of the Air Pollution Control Association. Montreal, Quebec: June 22-27, 1980. 2-16., 1980, 2-16.

Roulston, C., Paton-Walsh, C., Smith, T., Guérette, É. A., Evers, S., Yule, C. M., Rein, G., and Van der Werf, G.: Fine particle emissions from tropical peat fires decrease rapidly with time since ignition, Journal of Geophysical Research: Atmospheres, 123, 5607-5617, https://doi.org/10.1029/2017JD027827, 2018.

Stockwell, C. E., Jayarathne, T., Cochrane, M. A., Ryan, K. C., Putra, E. I., Saharjo, B. H., Nurhayati, A. D., Albar, I., Blake, D. R., and Simpson, I. J.: Field measurements of trace gases and aerosols emitted by peat fires in Central Kalimantan, Indonesia, during the 2015 El Niño, Atmospheric Chemistry and Physics, 16, 11711-11732, 2016.

Urbanski, S.: Wildland fire emissions, carbon, and climate: Emission factors, Forest Ecology and Management, 317, 51-60, https://doi.org/10.1016/j.foreco.2013.05.045, 2014.
Yokelson, R. J., Burling, I., Gilman, J., Warneke, C., Stockwell, C., Gouw, J. d., Akagi, S., Urbanski, S., Veres, P., and Roberts, J.: Coupling field and laboratory measurements to estimate the emission factors of identified and unidentified trace gases for prescribed fires, Atmospheric Chemistry and Physics, 13, 89-116, 2013.